Osseointegration of Titanium Implants With Different Rough Surfaces: A Histologic and Histomorphometric Study in an Adult Minipig Model

Massimo Del Fabbro, BSc, PhD,* Silvio Taschieri, MD, DDS,† Elena Canciani, BMT, PhD,‡ Alessandro Addis, DVM,§ Federica Musto, DDS,¶ Roberto Weinstein, MD, DDS,|| and Claudia Dellavia, DDS, PhD

Background: *Many chemical and physical modifications of titanium surfaces were introduced, aiming at improving surface bioactivity, but few comparative evidence exists.*

Objective: *To evaluate histologically in minipigs the osseointegration of implants made of commercially pure (CP) titanium or titanium alloy, treated by different roughening procedures.*

Material and Methods: *Three sandblasted acid-etched (SA) surfaces, 2 anodized (AN), and 1 double acid-etched (DAE) were compared. Surface microtopography was characterized with scanning electron microscope; surface element composition was also assessed. One implant per group was inserted in each proximal tibia of 2 minipigs. Three months after healing, block biopsies were taken for histomorphometric analysis. Implant stability quotient (ISQ) was measured at insertion and before harvesting.*

Results: *The highest amount of cortical bone-implant contact was observed around SA implants and showed positive correlation with surface roughness. The greatest increase in ISQ was observed in CP-AN implants. In the medullary region, SA implants showed the best osteogenic response, whereas inflammatory cells were found around DAE and alloy-AN implants.*

Conclusions: *SA surfaces were more osteogenic than anodized or dual acid-etched ones, although not significantly. Surface roughness affected osseointegration. (Implant Dent 2017;26:357–366)*

Key Words: animal model, bone healing, dental implants, implant surface

The use of titanium dental implants for the rehabilitation of edentulous patients has been one of the greatest breakthrough in dentistry, and its value is testified by a number of evidence-based studies reporting high long-term survival and success rates.[1] Since its introduction in the late 1960s, there has been an increasing expansion of the spectrum of clinical indications for implant therapy, and positive results have also been achieved in situations previously considered unfavorable such as in locally and systemically compromised patients. Among the factors mostly responsible for such evolution is the relevant progress made in the field of implant surfaces that has led to the development of a number of chemical and physical modifications of the traditional titanium surfaces, aiming at improving the bioactivity of the surface, the cross-talk with surrounding bone and ultimately its ability of eliciting and maintaining implant osseointegration.

Modern implant dentistry is more and more oriented toward the overall reduction of the treatment time, through early and immediate loading protocols for any type of prosthetic reconstruction.[2–5] Minimizing the number of surgical sessions, in addition to decreasing the treatment time, may also reduce morbidity, overall cost, and patient discomfort, increasing patient's acceptance of the implant

*Associate Professor, Department of Biomedical, Surgical and Dental Sciences, Università degli Studi di Milano, Milan, Italy; Head of Section of Oral Physiology, Dental Clinic, IRCCS Istituto Ortopedico Galeazzi, Milan, Italy.
†Academic Researcher, Department of Biomedical, Surgical and Dental Sciences, Università degli Studi di Milano, Milan, Italy; Head of Section of Endodontics, Dental Clinic, IRCCS Istituto Ortopedico Galeazzi, Milan, Italy.
‡Postdoc Fellow, Department of Biomedical, Surgical and Dental Sciences, Università degli Studi di Milano, Milan, Italy.
§Visiting Professor, Università degli Studi di Milano, Milan, Italy; CEO at CRABCC srl (Biotechnology Research Center for Cardiothoracic Applications), Rivolta d'Adda, Cremona, Italy.
¶PhD Student, Department of Biomedical, Surgical and Dental Sciences, Università degli Studi di Milano, Milan, Italy.
||Full Professor, Director of Department of Biomedical, Surgical and Dental Sciences, Università degli Studi di Milano, Milan, Italy. Head of Dental Clinic, IRCCS Istituto Ortopedico Galeazzi, Milan, Italy.
#Associate Professor, Head of the Ground Section Laboratory, Department of Biomedical, Surgical and Dental Sciences, Università degli Studi di Milano, Milan, Italy.

Reprint requests and correspondence to: Massimo Del Fabbro, BSc, PhD, Università degli Studi di Milano, IRCCS Istituto Ortopedico Galeazzi, Via Riccardo Galeazzi 4, 20161 Milano, Italy, Phone: +39 02 50319950, Fax: +39 02 50319960, E-mail: massimo.delfabbro@unimi.it

ISSN 1056-6163/17/02603-357
Implant Dentistry
Volume 26 • Number 3

DOI: 10.1097/ID.0000000000000560

treatment. In addition, a number of evidence-based systematic reviews of clinical studies showed that the outcome of implant treatment with early and immediate loading is as predictable as conventional delayed loading.[6–9] To successfully perform such protocols, the achievement of rapid and predictable implant osseointegration is mandatory. Among the many factors that may affect the latter, implant surface topography, in its microstructural and nanostructural aspects, represents a key element.[10–20] It is since long well established that textured surfaces allow to accelerate the process of osseointegration of implants due to the so-called phenomenon of *contact osteogenesis*, in which new bone is formed starting directly from the implant surface.[21–23] Such process has not been observed with traditional machined-surface implants, whose osseointegration is typically characterized by the *distance osteogenesis* in which bone formation occurs centripetally from the old bone surface toward the implant surface in an appositional manner.[21–24] Contact osteogenesis may lead to bone bonding if the implant surface possesses the appropriate topography.[25] In the recent years, many different implant surfaces have been introduced, having microtopographic and nanotopographic features obtained with different production techniques, with the aim of enhancing the osseointegration process.[18,26,27] Such types of textured surfaces may affect in different ways the osseous healing process at the implant-bone interface, modulating quality and quantity of neo-formed periimplant bone. The early stages of peri-implant bone healing are critical and involve the host's initial response to a foreign material: protein adsorption, platelet activation, coagulation, and inflammation.[28–30] This leads to the formation of a stable fibrin clot, which acts a storage for growth factors and cytokines and allows for osteoconduction. The latter consists of the migration and differentiation of osteogenic cells, such as pericytes, into osteoblasts that ultimately produce bone matrix. Osteoconduction allows for contact osteogenesis to occur at the implant surface, as osteoblasts are able to migrate through the fibrin matrix until reaching the implant. The late stage of periimplant bone healing involves the remodeling of the early synthesized woven bone. In addition to understanding how periimplant bone formation begins, it is as well important to assess how different osteoconductive surfaces are integrated in the bone once the early healing process has occurred, which is fundamental to the prognosis of the implant-supported reconstruction.

The purpose of the present study was to evaluate histologically and histomorphometrically the osseointegration of titanium implants with textured surface, according to the material composition (titanium degree), and the type of treatment applied to roughening surface, after 3 months of submerged healing in the minipig tibia model.

MATERIAL AND METHODS

Two female Yucatan minipigs, 3 years old and weighing on the average 45 to 50 kg were used. All the experimental procedures were conducted in accordance with the current Italian law D.Lg 26-14 and the European regulatory 2010/63/UE for the use of animals in scientific research. The study received ethical approval by the Italian Ministry of Health. The animals were hosted 1 per cage with food and water *ad libitum* in standard conditions of light, temperature, and humidity (12 hours a day; 20°C; 50% ± 5%). Before the experimental procedure, animals had an acclimation and an observation period of 10 days.

Titanium Implants

Twenty-four titanium implants having the same size, shape, and thread pattern so as to be macroscopically equivalent, were divided into 6 groups according to their surface texture and titanium degree (4 or 5). Degree 4 titanium is commercially pure (CP) titanium, whereas degree 5 is an alloy (Ti6Al4V) composed of 6% alumina, 4% vanadium, up to 0.25% iron, up to 0.2% oxygen, and the remaining about 89.6% titanium.

The different surfaces compared were as follows:

1. Blasted Wrinkled Surface (BWS; commercial implant produced by Dental Tech, Misinto, Milan, Italy): implants made of titanium alloy undergoing sandblasting with pure aluminum oxide and subsequent etching with nitric and fluoridric acid;
2. Hydroxyapatite (HA) (commercial implant produced by Dental Tech): implants made of CP titanium undergoing sandblasting with HA and subsequent etching with nitric acid;
3. Double acid etching (DAE; prototype produced by Politecnico, Milan, Italy): implants made of titanium alloy undergoing DAE process. The first etching is obtained submerging implants in fluoridric acid, then implants are etched with a combination of chlorhydric and sulfuric acid (HCl/H_2SO_4); finally implants are heated at 60°C to 80°C for 3 to 10 minutes.
4, 5. Anodic spark deposition (ASD; prototypes produced by Eurocoating, Ciré-Pergine, Trento, Italy): implants undergoing anodic polarization up to 300 V or more, depending on the type of electrolyte in solution (eg, Si, Ca, P, Na). A titanium oxide film is formed at the surface that progressively acquires microporous features characterizing implants with a moderate roughness. It is not a surface coating but a thickening and modification of the oxide layer naturally present at the implant surface. Implants made of both CP titanium and titanium alloy underwent such surface treatment and were used in 2 separate groups.
6. SLA (prototype produced by Nobil Bio Research, Concesio, Brescia, Italy): implants made of CP titanium undergoing sandblasting with large-grit aluminum oxide (Al_2O_3) particles, that creates a macrorugosity of the surface, followed by strong acid etching with chlorhydric and sulfuric acid (HCl/H_2SO_4)

at elevated temperature for several minutes. The latter produces microrugosity (2–4 μm micropits) superimposed to the rough-blasted surface.

Surface Analysis of Implants

Implant surface microtopography of the implants used in the study was analyzed by scanning electron microscope (SEM) (VEGA; Tescan, Brno, Czech Republic) (Fig. 1, A–C). The main parameters adopted to characterize implant surface roughness were measured: eg, mean Ra (average roughness of the profile), Sa (average height of selected area), Sdr (developed interfacial area ratio). Linear assessments were made along a 1-mm-long continuous line. Surface assessments were based on an area of about 200 × 200 μm. The surface element composition of each implant was also determined using an energy-dispersive x-ray microanalyzer unit (QUANTAX EDS; Bruker Italia, Milan, Italy) combined with the SEM (Fig. 2).

Animal Models

Each minipig received 6 standard implants of 4 mm diameter × 8 mm length per each tibia. A total of 24 implants (12× animal) were inserted and were divided in 6 groups (n = 4) as follows: group 1: BWS; group 2: HA; group 3: DAE; group 4: ASD T5 (Ti alloy); group 5: ASD T4 (CP Ti); group 6: SLA.

Surgical Procedure

Before the surgical procedures, a fasting of 10 hours was observed and all animals received the same anesthetic and analgesic protocol. Preanesthesia consisted in intramuscular injection of ketamine10 mg/kg and midazolam 0.5 mg/kg. The auricular vein of each animal was catheterized for the Ringer lactate solution infusion. Anesthesia was obtained via an oronasal mask with a mixture of isoflurane 4.5% and oxygen and after the intubation with the orotracheal tube no. 7, anesthesia was maintained with 3.5% isoflurane, 100% O_2. Intraoperative analgesia was provided with tramadol (1 mL/kg IV) and meloxicam (0.4 mg/kg).

Surgery was performed under standard aseptic conditions following a standard procedure: after disinfection of the surgical site, skin, subcutis, underlying muscles, and periosteum were longitudinally sectioned to expose proximal tibial crest. Six implant sites of 4-mm diameter were prepared in each tibia using standard surgical drills. Each implant was randomly inserted supracrestal or at the level of the tibial crest along the tibial longitudinal axis at a distance of 4 to 5 mm from each other. The implant type allocation along the longitudinal axis of the tibia was randomly assigned according to a computer-generated sequence. A minimum insertion torque of 25 N cm was achieved. Figure 3 is a picture of the surgical site showing the implants soon after placement in the tibia. After application of the cover screws, the surgical fascia was closed using a monofilament synthetic absorbable suture in Poliglecaprone 25 (Monocryl 4-0 USP) and the skin was sutured in separate layers using a nonabsorbable synthetic suture in polypropylene (Prolene 3-0 USP). The skin sutures were removed 14 days later.

After surgery, the animals were recovered and stabilized in the same preoperative condition for 12 weeks. To prevent infection, the animals received marbofloxacin (Marbocyl 2 mg/kg intravenously) and long-acting amoxicillin (Terramycin/LA 15 mg/kg intramuscularly) at the time of surgery. An antibiotic prophylaxis with 5 mg/kg enrofloxacin (Baytril sol. 2.5%) was given intramuscularly (IM) for 5 days following surgery to prevent infections and analgesics meloxicam (Metacam 0.4 mg/kg IM) were administered for 4 days. During this follow-up period, specialized veterinary staff visited the animals periodically for early detection of pain or

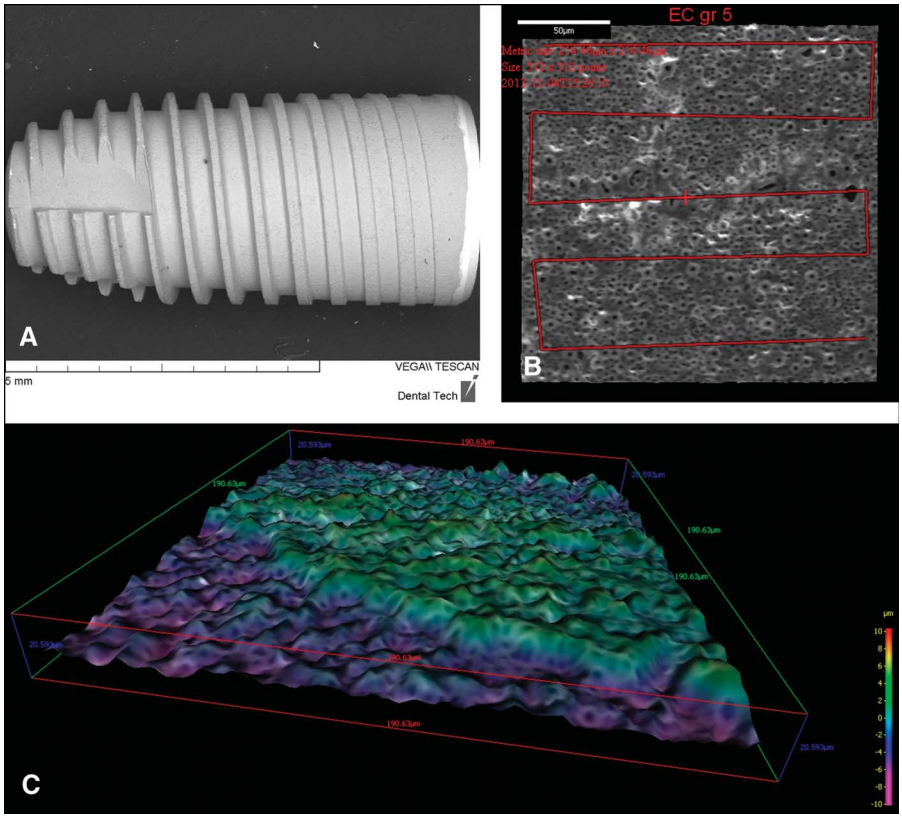

Fig. 1. Surface evaluation with SEM of an implant made of titanium alloy undergoing anodic oxidation (group ASD-T5). **A**, Low-resolution overview of the implant (image obtained with back-scattering), magnification ×40. **B**, Image showing the red line used to measure Ra, bar = 50 μm. **C**, Three-dimensional reconstruction of the surface, used to measure Sdr.

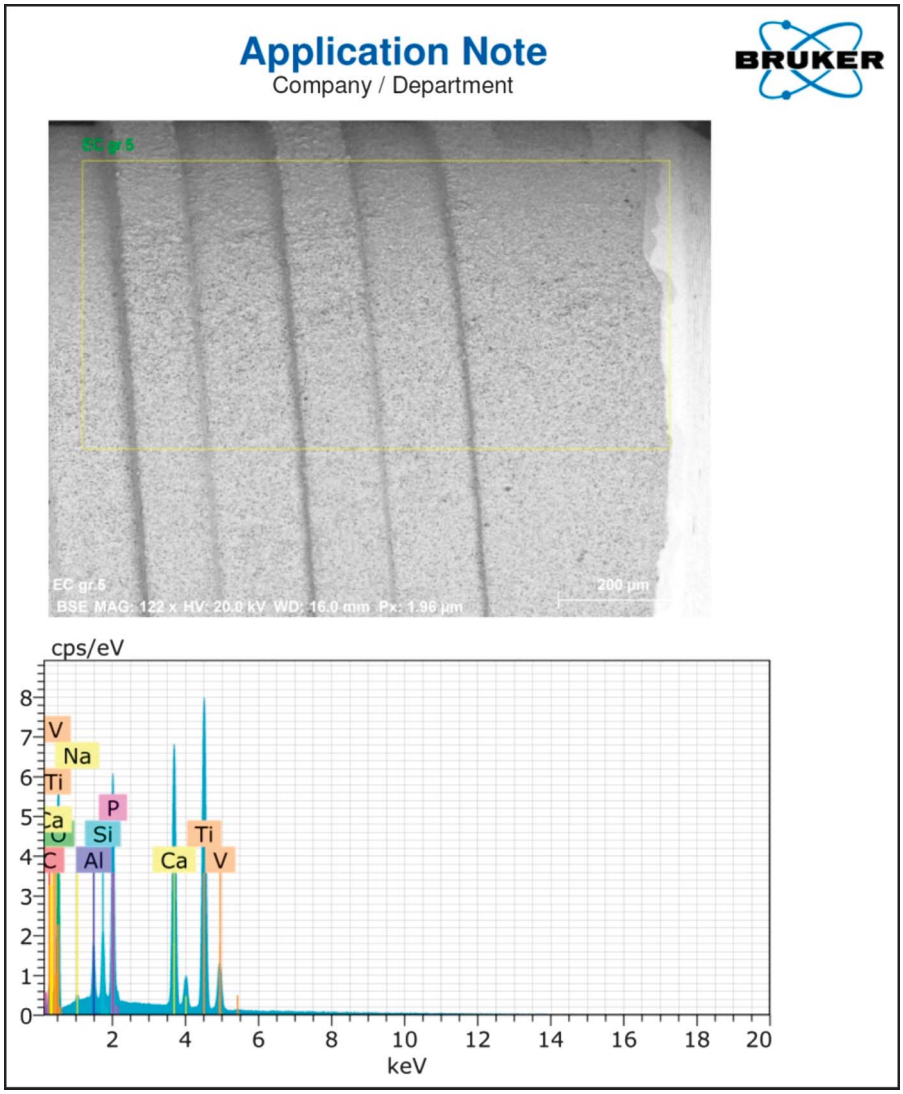

Fig. 2. An example of the surface element composition with EDS. This evaluation refers to an implant made of titanium alloy undergoing anodic spark deposition (ASD-T5 group). Top: The area of implant surface undergoing spectroscopic analysis; magnification ×122, bar = 200 μm. Bottom: EDS spectrum of the surface element composition. Peaks relative to the amount of the various elements present on the surface are visible and distinct. The most abundant are O, Ti, Ca, whereas Na, V, Al, and Si are only present in traces (<2%).

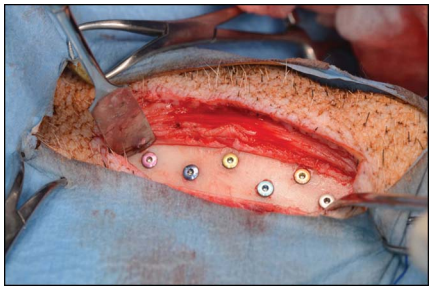

Fig. 3. Picture of the surgical site taken after random sequential placement of all implant types in the minipig tibia. Each group was characterized by a different color of the cover screw. In the specific case, from the proximal end of the right tibia (right side on the image) to the distal one (left) they were as follows: ASD-T4, DAE, BWS, ASD-T5, HA, SLA.

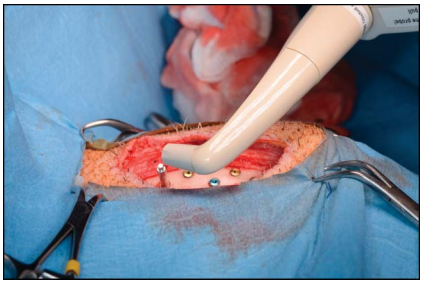

Fig. 4. ISQ was measured with Osstell Mentor device at implant insertion. The Smartpeg was screwed into an implant belonging to HA group and tightened at 5 N cm. The white transducer probe with a curved end was positioned as close as 2 to 3 mm to the top of the Smartpeg and firmly held until the device measured the impulse and displayed the ISQ value, that in the specific case was 80.

any clinical sign or symptom of discomfort, and daily intake of food and water was recorded. In case of detection of any behavior indicating discomfort, the veterinary staff would have immediately informed the principal investigator and an appropriate therapy undertaken to manage the problem and, in case no therapeutic option could have been used or proved effective to address the issue, the animals would have been euthanized. After 12 weeks, all animals were humanely killed with intravenous overdose of potassium chloride, after induction of general anesthesia as described previously.

Implant Stability Quotient Evaluation

The stability of each implant was measured through a resonance frequency analysis device (Osstell Mentor; Integration Diagnostics AB, Göteborg, Sweden). A Smartpeg (Integration Diagnostics AB) was screwed into each implant and tightened to approximately 5 N cm. The transducer probe was aimed at the small magnet at the top of the Smartpeg at a distance of 2 or 3 mm and held stable during the pulsing until the instrument beeped and displayed the implant stability quotient (ISQ) value (Fig. 4). The ISQ values were measured soon after insertion in the proximal tibia (baseline) and after 3 months, just before removal of bone blocks from tibiae after killing the animals. The measurements were taken twice in the buccolingual direction and twice in the mesiodistal direction. The mean of the 2 highest measurements from each direction was regarded as the representative ISQ of that implant.

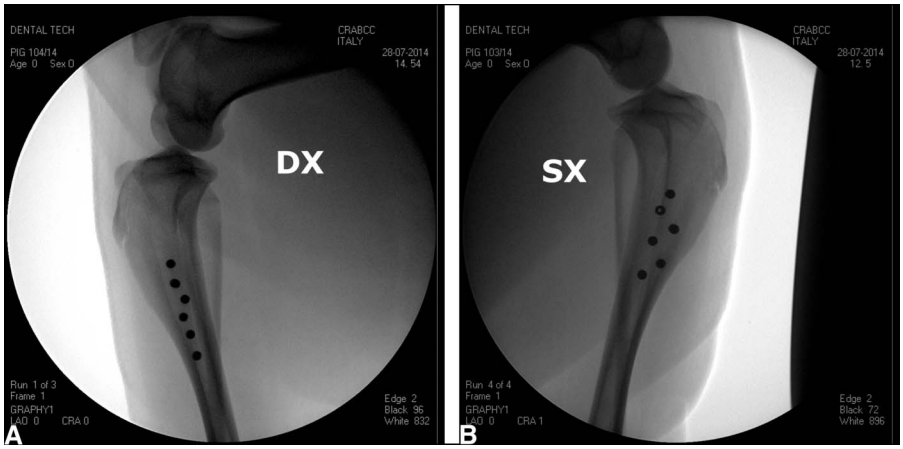

Fig. 5. Radiographs of the tibiae (one for each animal) taken soon after random sequential placement of one implant per group in each tibia minipig. **A**, From the proximal side (top) to the distal one (bottom) of the right tibia the sequence is as follows: BWS, ASD-T5, ASD-T4, DAE, SLA, HA. **B**, From the proximal side (top) to the distal one (bottom) of the left tibia the sequence is as follows: DAE, ASD-T4, ASD-T5, BWS, SLA, HA.

Radiographic Examination

The tibiae of the animals underwent conventional radiographic evaluation after the surgical procedure to assess proper implant positioning (Fig. 5). Radiographs were also taken before bone blocks removal after killing the animals (Fig. 6) using a digital radiography system Fujifilm D-EVO model.

Fig. 6. Radiograph of the tibiae of one minipig after explantation (3 months after surgery). Here one can appreciate parallelism among implants. Left: from top to bottom of the left (SX) tibia the sequence was: ASD-T5, BWS, DAE, ASD-T4, HA, SLA; right: from top to bottom of the right (DX) tibia the sequence was: BWS, ASD-T5, ASD-T4, DAE, SLA, HA.

Histological and Histomorphometric Analysis

After killing, wide bone block biopsies including 6 implants were harvested from each experimental region of the tibia and placed in fixative (4% formalin). Subsequently, a small dissection saw was gently used to cut 24 blocks containing 1 implant each. For this procedure, no trephine bur was used because vibrations could have damaged the implant-bone interface. The samples were preserved in 4% formalin (pH = 7), dehydrated in increasing alcohol scale (70, 80, 90, 96, and 100%), infiltrated in alcohol resin in decreasing ratio (3 alcohol:1 resin, 1:1, 1:3, pure resin), and finally embedded in pure methyl-methacrylate resin (Technovit7200 VLC, Exact Kultzer; Bio-Optica, Milano, Italy). Samples were then sectioned longitudinally using a precision sectioning saw with dedicated diamond blade (Micromet; Remet, Bologna, Italy). Sections were then ground and polished to a final thickness of 80 μm using a microgrinding unit (LS2; Remet). From each tissue block, 2 sections were obtained, stained in toluidine blue/Pyronin G (Sigma-Aldrich, St Louis, MO), and observed using a light microscope (Eclipse E600; Nikon, Tokyo, Japan) equipped with a calibrated digital camera (DXM1200; Nikon). All aspects of each section were photomicrographed at a magnification of ×10 and were merged to obtain the whole image using an image analyzer (Rhinoceros NURBS modeling for Windows, version 3.0; McNeel, Seattle, WA). On each reconstructed image, a histomorphometric examination was performed. Bone-to-implant contact (BIC) was measured in a standardized coronal region for all implants at the level of cortical bone. In the apical region, BIC was qualitatively evaluated, due to the inhomogeneity of medullar bone around implants. The presence of bone matrix at the implant surface was scored as A (more than 75% of the observed surface had contact with bone tissue), B (between 50% and 75%), C (between 25% and 50%), and D (lower than 25%).

Statistical Analysis

Data of quantitative variables were synthesized by mean values and standard deviations. Nonparametric tests were used for comparisons. Kruskal-Wallis test was used to evaluate between-group differences, and Wilcoxon matched-pairs signed-rank test was used to compare groups, two at a time. Pearson' correlation between the main surface roughness parameters

Table 1. Surface Parameters

	ASD T4	ASD T5	BWS	HA	SLA	DAE
Ra (μm)	1.3251	1.1603	1.6317	2.1615	2.2528	1.472
Sa (μm)	1.1814	1.0696	1.472	2.0828	1.5469	1.3461
Sdr (%)	54.84	38.97	71.70	170.76	88.99	66.37

Results of the implant surface microtopography evaluation performed with SEM. The parameters are expressed as mean values. Ra indicates mean height of the profile along a 1-mm line; Sa, mean height of the profile along a selected area (about 200 × 200 μm); Sdr, mean interfacial extension of a selected area (about 200 × 200 μm) with respect to the linear surface area; eg, a value of 50% means that the measured extension of the rough surface on a selected area is 50% greater compared with a flat surface having the same selected area.

Table 2. Results of the EDS Analysis: Mean (Standard Deviation) Percentage of Elements and at the Implant Surface

Element	ASD T4	ASD T5	BWS	HA	SLA	DAE
Ti	26.59 (0.79)	24.79 (0.79)	87.19 (2.12)	96.19 (2.38)	90.51 (2.34)	85.77 (2.17)
O	50.97 (6.46)	47.68 (6.00)	2.39 (0.27)	—	5.44 (1.05)	—
C	3.48 (0.69)	4.60 (0.85)	1.91 (0.12)	3.81 (0.63)	4.06 (0.68)	4.05 (0.70)
Al	—	1.60 (0.11)	4.77 (0.42)	—	—	6.23 (0.30)
V	—	0.61 (0.05)	2.53 (0.09)	—	—	2.61 (0.10)
Na	0.70 (0.08)	0.64 (0.07)	—	—	—	—
Si	1.45 (0.09)	1.54 (0.09)	—	—	—	—
P	5.63 (0.25)	6.01 (0.26)	—	—	—	—
Ca	11.17 (0.37)	12.54 (0.40)	—	—	—	—
N	—	—	1.19 (0.28)	—	—	1.34 (0.31)

The surfaces treated by anodic spark deposition showed the highest enrichment of elements as Na, Si, P, Ca on their surface. Implants made of titanium alloy (groups ASD-T5, BWS, DAE) showed the presence of Ti and Al, the elements characteristics of the alloy, in addition to Ti.

and BIC and between ISQ and BIC was performed. $P = 0.05$ was considered as the significance level.

RESULTS

No complications occurred during the follow-up period.

Surface Characterization

In Table 1 are reported the main surface parameters for each type of implant. The surface displaying the highest average roughness of the profile was the SLA (Ra = 2.25 μm), whereas the HA had the greatest average height of selected area (Sa = 2.08 μm), and the far greatest developed interfacial area ratio (Sdr), with an extension of 170% more as compared with flat surface. Table 2 reports the results of the surface element composition analysis for each group.

Implant Stability

Regarding implant stability, after 3 months of healing, all implants showed an increase of the mean ISQ value compared with baseline evaluation, except for implants with DAE surface that showed a slight, not statistically significant reduction. The mean data with standard deviations are reported in Table 3. The greatest increase in ISQ was observed in group ASD-T4 (13.3% more respect to baseline), followed by groups ASD-T5 and SLA (both had an 11.2% increase of ISQ). However, no difference achieved statistically significance, also due to a nonnegligible within-group variability.

Histologic and Histomorphometric Analysis

In all groups, a satisfactory bone healing was observed, with new bone formation along the bone-implant interface. In Figure 7, A examples of histological sections of the 6 implant types are shown at low magnification (×4). Figure 7, B displays pictures at higher magnification (×20) showing new bone formation between implant threads at the level of the cortical bone. All the implants appeared to be osseointegrated in the newly formed bone without gaps between the implant surface and newly formed tissue. The inflammatory infiltrate was not detected.

In Table 4 are shown the mean values of BIC measured at the coronal portion of the implants at the level of the cortical bone. After 3 months, the highest mean BIC value was observed for the HA surface, followed by the BWS, SLA, and ASD-T5, all higher than 80%, whereas the lowest BIC was found for the dual acid-etched surface.

Kruskal-Wallis test did not show significant differences among groups ($P = 0.48$). When comparing 2 groups at a time using Wilcoxon matched-pairs signed-rank test, no difference achieved statistical significance.

When correlating coronal BIC values with the main surface parameters, and with resonance frequency analysis results, a modest positive correlation was observed between BIC and Sa and between BIC and Sdr (correlation coefficient r = 0.63 in both cases). A lower positive correlation was found between BIC and Ra (r = 0.53), and even lower between BIC and ISQ (r = 0.38 at baseline and r = 0.51 at 3 months).

Regarding the apical portion of the implants in the medullary portion of the tibial bone shown in Figure 7, C at high magnification (×20), as said above, a quantitative evaluation was not feasible and only qualitative assessment of the newly formed tissue was done. For implants with SLA surface, in the medullary region, a thin layer of bone matrix was uniformly present in contact with implant surface, and the score was A. For DAE surface, a bone matrix with different degrees of maturation was observed

Table 3. Mean ISQ

	ASD T4	ASD T5	BWS	HA	SLA	DAE
ISQ baseline	65.9 ± 9.0	69.0 ± 9.4	66.50 ± 9.1	72.5 ± 6.5	70.5 ± 9.9	69.3 ± 7.6
ISQ 3 mo	74.6 ± 2.7	76.8 ± 2.8	72.8 ± 6.0	73.3 ± 9.9	78.4 ± 2.6	68.3 ± 6.1
P-value	0.12	0.24	0.19	0.94	0.29	0.89

The measurement technique is described in the text. Values are expressed as mean ± standard deviation.

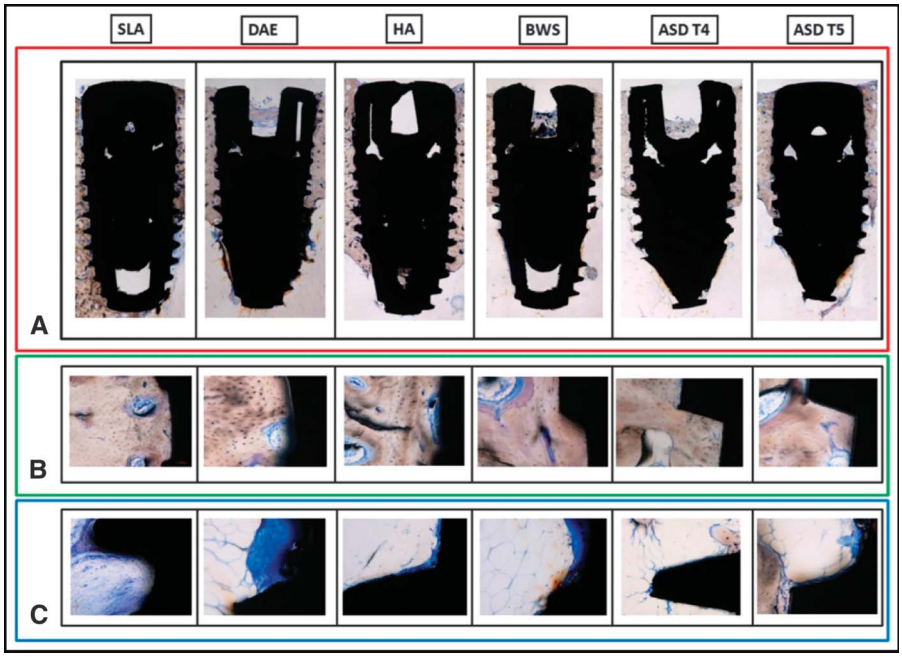

Fig. 7. Histological sections of the 6 different implant types. The groups are indicated at the top side. One implant per group is shown in each panel. **A**, Overview at low magnification (×4) of the whole body of the implant integrated to the minipigs tibial bone. Samples were stained with toluidine blue and Pyronin G (yellow). **B**, Higher magnification (×20) of a portion of the implants taken at the level of the cortical bone. This region was used to assess the bone-to-implant contact, as described in the text. Samples were stained with toluidine blue and Pyronin G (Yellow). **C**, Higher magnification (×20) of a portion of the implants taken in the medullary region of the tibial bone. This region was used for the qualitative evaluation of bone healing around the apical side of the implants. Samples were stained with toluidine blue and Pyronin G (yellow).

along the surface, with some regions thicker than others. The presence of inflammatory cells was observed in some periimplant regions; the score for DAE surface was B. In the group with HA surface, newly formed bone from surrounding trabeculae directed toward and adhered to implant surface, forming a rather thick layer with zones at high concentration of osteoblast-like cells. The score for bone matrix was B. Newly formed bone around implants of the group BWS appeared very similar to HA, with deposited matrix rather thick (although with variable thickness and density), and containing a high osteoblasts concentration. Bone matrix score was B.

For implants ASD-T4, new bone projecting from adjacent trabeculae appeared to be directed toward the implant surface, but less actively and with lower matrix formation as compared with the previous cases. Matrix layer was very thin and discontinuous, sometimes it lacked adherence displaying a tent effect. The score for matrix contacting bone was C. The aspect of bone matrix in group ASD-T5 around the apical implant region was similar to ASD-T4, but in zones where adherence was lacking, the presence of some inflammatory cells close to implant surface was observed in both animals. Bone matrix score was C.

Table 4. Mean and SD of BIC in the Coronal Region

	ASD T4	ASD T5	BWS	HA	SLA	DAE
Mean	79.02	80.50	81.59	83.53	80.79	76.05
SD	9.46	6.77	5.67	4.10	5.61	3.53

SD, standard deviation.

DISCUSSION

Among the advantages of the minipig model used in the present study, there is the possibility of testing simultaneously different implant surfaces for their ability of inducing osseointegration, that is the capacity of bone to form rigid and stable load-bearing anchorage to implants. To reduce the effect of the variation in the thickness of cortical bone of the tibia on osseointegration, the sequence of implants along the proximal-distal direction was changed randomly at placement. In addition, the BIC was evaluated within a standard distance of 1 mm at the coronal level, so as to allow comparison among all implants.

With regard to bone anatomy, morphology, healing, and remodeling, the minipig model is considered to be closely representative of human bone and therefore a suitable species of choice.[31–33] Regarding the bone microstructure, the minipig has denser trabecular network than human bone, but lamellar bone structure is similar to that of humans.[34] Porcine bone also has similarities in bone mineral density and concentration with respect to human bone,[35] and the structure, composition, and density of minipig tibia is rather similar to the human mandibular bone.[36] Furthermore, minipigs and pigs have bone remodeling processes similar to humans, including both trabecular and intracortical bone multicellular unit– based remodelling.[34,37] Finally, a study on the effects of fluoride on cortical bone remodeling in growing pigs showed that in control animals the cortical bone mineralization rate is comparable with humans.[38] The minipig tibia model has been used previously in several studies evaluating novel implant design or surfaces.[36,39–43]

In the present study, we were particularly interested in assessing the degree of osseointegration and the quality of the newly formed periimplant bone after completion of the early phases of osseointegration. This reflects the condition usually encountered when prosthetic phase is performed in conventional implant treatment, after periimplant bone

healing in the submerged mode. The quality and quantity of the bone surrounding implants at the time of loading in fact is a critical factor to the prognosis of the implant-supported reconstructions. Ideally, the highest possible amount of BIC should be present at the interface with cortical bone, which gives the necessary stability and support to the implant under function, and no signs of inflammation should be detected in the adjacent tissues. Indeed, the presence of low-level infiltration of lymphocytes around the implants at the early stage of the osseointegration process may be interpreted as a factor favorable to promoting osteogenesis, as it is well known that the presence of inflammatory cells correlates with growth factors production and mesenchymal stem cells recruitment.[44–46] Such infiltrates, however, should virtually disappear once the implant integration process is completed, and the late detection of infiltration might indicate the persistence of an inflammatory stimulus at the interface, with a possible delay in the formation of mature bone around implants. In the present study, inflammatory cells were clearly detected after 3 months of healing around implants with oxidized surface made of titanium alloy (but not around implants made of CP titanium undergoing the same surface treatment), and in a lesser degree, around implants with DAE surface, also made of titanium alloy. Such findings are difficult to explain, they could be possibly related to a given combination of superficial elements in a given proportion that might induce some kind of tissue response.

In fact, beside surface texture, the chemistry of implant surface may play a role in driving the biological mechanisms at the interface.[47,48] For instance, Varoni et al[49] suggested that the Poly-L-lysine coating of titanium implants safely promotes osteoblast calcium position and periimplant cortical bone hardness in ovine model. The ionic composition at implant surface may be determined by the fixture material (CP titanium or alloy) by the surface treatment used for achieving the desired roughness, as well as by the manufacturing and polishing process, which may leave residual contaminant elements on the surface. Such elements, either present in a relevant percentage or in traces, may affect the biological processes and in some cases elicit some kind of host reaction.[50,51] No significant difference in osseointegration was found according to the bulk material implants are made, that is CP titanium or alloy implants, in agreement with previous studies.[52,53] In the present study, some differences in surface composition were observed by EDS assessment among groups as shown in Table 3. No association could be observed between BIC at coronal level and implant material or surface composition. It is worth noting that the aforementioned signs of inflammation at the apical level, could not be correlated to a particular element or combination of elements detected at the surface, although the number of samples is still too low to hypothesize a significant trend. However, it was not an aim of the present study to investigate such topic, it could be specifically addressed in future investigations.

Regarding the correlation between surface roughness and osseointegration, a number of experimental studies have demonstrated that the periimplant bone response is influenced by the implant surface topography.[13,16,54] Albrektsson and Wennerberg in 2004 defined a classification of implant surface roughness based on Sa, scoring the surfaces into smooth (Sa <0.5 μm), minimally rough (Sa from 0.5 to 1 μm), moderately rough (Sa from 1 to 2 μm), and rough (Sa >2 μm).[55] Although it is clear that smooth and minimally rough surfaces show a less strong bone response than rougher surfaces, no clear superiority has been demonstrated between moderately rough and rough surfaces, with the former displaying better results in some studies. The comparison between different studies however has some limitations because of the varying quality in the surface assessment techniques and different definitions of surface roughness adopted in different studies.[13,55] Although it has been claimed that nanostructured surfaces might positively influence bone response, a systematic review of the available evidence by Wennerberg and Albrektsson showed that no clear indication exists that implants with such topography at the nanometer level are associated with superior osseointegration, better implant survival, and reduced periimplant bone loss as compared wtih implants with surface topography at the micrometric level.[13] Therefore, in the present study, micrometric assessment of the implant surface was made and results were correlated to the surface roughness parameters on a micrometric scale, although some of the implant treatment might have created surface irregularities in the nanometric range. The present analysis showed that all implant types achieved a good degree of osseointegration at cortical level, being the highest BIC values associated with the highest values of profile roughness at linear (Ra) and surface (Sa) level, and of interfacial area ratio (Sdr). Implants with moderately rough surface, like those in the ASD groups, and especially those treated by dual acid etching, characterized by lower values of Ra, Sa, and Sdr than other groups, displayed the lower BIC values. These results further support the hypothesis that a correlation may exist between the degree of surface roughness and the ability of an implant to achieve a high degree of osseointegration after completion of the healing process.

CONCLUSIONS

In the minipig tibia model with all implants in the same conditions, based on the histological and histomorphometric outcomes the surfaces produced through a sandblasting plus acid-etching procedure achieved nonsignificantly better outcomes than those undergoing anodic oxidation or dual acid etching. Osseointegration was positively correlated to the roughness degree of the implant surface.

DISCLOSURE

The authors claim to have no financial interest, either directly or

indirectly, in the products or information listed in the article.

APPROVAL

All the experimental procedures were conducted in accordance with the current Italian law D.Lg 26-14 and the European regulatory 2010/63/UE for the use of animals in scientific research. The study received Ethical approval by the Italian Ministry of Health.

ACKNOWLEDGMENTS

The authors thank Dental Tech Srl (Misinto, Milan, Italy) for providing the implants, the technology for surface evaluation, and for partially funding the study.

REFERENCES

1. Moraschini V, Poubel LA, Ferreira VF, et al. Evaluation of survival and success rates of dental implants reported in longitudinal studies with a follow-up period of at least 10 years: A systematic review. *Int J Oral Maxillofac Surg.* 2015;44:377–388.

2. Bahat O, Sullivan RM. Parameters for successful implant integration revisited part I: immediate loading considered in light of the original prerequisites for osseointegration. *Clin Implant Dent Relat Res.* 2010;12(suppl 1):e2–e12.

3. Esposito M, Grusovin MG, Polyzos IP, et al. Timing of implant placement after tooth extraction: Immediate, immediate-delayed or delayed implants? A cochrane systematic review. *Eur J Oral Implantol.* 2010;3:189–205.

4. Joshi N, Joshi M, Angadi P. Immediate loading of dental implants: Review of the literature. *J Long Term Eff Med Implants.* 2011;21:269–279.

5. Delben JA, Goiato MC, Pellizzer EP, et al. Planning for immediate loading of implant-supported prostheses: Literature review. *J Oral Implantol.* 2012(38 spec no):504–508.

6. Romanos G, Froum S, Hery C, et al. Survival rate of immediately vs delayed loaded implants: Analysis of the current literature. *J Oral Implantol.* 2010;36:315–324.

7. Strub JR, Jurdzik BA, Tuna T. Prognosis of immediately loaded implants and their restorations: A systematic literature review. *J Oral Rehabil.* 2012;39:704–717.

8. Esposito M, Grusovin MG, Maghaireh H, et al. Interventions for replacing missing teeth: Different times for loading dental implants. *Cochrane Database Syst Rev.* 2013:CD003878.

9. Sanz-Sanchez I, Sanz-Martın I, Figuero E, et al. Clinical efficacy of immediate implant loading protocols compared to conventional loading depending on the type of the restoration: A systematic review. *Clin Oral Implants Res.* 2015;26:964–982.

10. Triplett RG, Frohberg U, Sykaras N, et al. Implant materials, design, and surface topographies: Their influence on osseointegration of dental implants. *J Long Term Eff Med Implants.* 2003;13:485–501.

11. Abrahamsson I, Berglundh T, Linder E, et al. Early bone formation adjacent to rough and turned endosseous implant surfaces. An experimental study in the dog. *Clin Oral Implants Res.* 2004;15:381–392.

12. Burgos PM, Rasmusson L, Meirelles L, et al. Early bone tissue responses to turned and oxidized implants in the rabbit tibia. *Clin Implant Dent Relat Res.* 2008;10:181–190.

13. Wennerberg A, Albrektsson T. Effects of titanium surface topography on bone integration: A systematic review. *Clin Oral Implants Res.* 2009;20:(suppl 4):172–184.

14. Wennerberg A, Albrektsson T. On implant surfaces: A review of current knowledge and opinions. *Int J Oral Maxillofac Implants.* 2010;25:63–74.

15. Dohan Ehrenfest DM, Coelho PG, Kang BS, et al. Classification of osseointegrated implant surfaces: Materials, chemistry and topography. *Trends Biotechnol.* 2010;28:198–206.

16. Gupta A, Dhanraj M, Sivagami G. Status of surface treatment in endosseous implant: A literary overview. *Indian J Dent Res.* 2010;21:433–438.

17. Orsini E, Salgarello S, Martini D, et al. Early healing events around titanium implant devices with different surface microtopography: A pilot study in an in vivo rabbit model. *ScientificWorldJournal.* 2012;2012:349842.

18. Grandfield K, Gustafsson S, Palmquist A. Where bone meets implant: The characterization of nano-osseointegration. *Nanoscale*. 2013;5:4302–4308.

19. Aljateeli M, Wang HL. Implant microdesigns and their impact on osseointegration. *Implant Dent.* 2013;22:127–132.

20. Annunziata M, Guida L. The effect of titanium surface modifications on dental implant osseointegration. *Front Oral Biol.* 2015;17:62–77.

21. Davies JE, Hosseini MM. Histodynamics of endosseous wound healing. In: Davies JE, ed. *Bone Engineering*. Toronto, Canada: Em Squared Inc; 2000:1–14.

22. Davies JE. Understanding peri-implant endosseous healing. *J Dent Educ.* 2003;67:932–949.

23. Kuzyk PR, Schemitsch EH. The basic science of peri-implant bone healing. *Indian J Orthop.* 2011;45:108–115.

24. Carmagnola D, Botticelli D, Canciani E, et al. Histologic and immunohistochemical description of early healing at marginal defects around implants. *Int J Periodontics Restorative Dent.* 2014;34:e50–e57.

25. Kieswetter K, Schwartz Z, Dean DD, et al. The role of implant surface characteristics in the healing of bone. *Crit Rev Oral Biol Med.* 1996;7:329–345.

26. Goené RJ, Testori T, Trisi P. Influence of a nanometer-scale surface enhancement on de novo bone formation on titanium implants: A histomorphometric study in human maxillae. *Int J Periodontics Restorative Dent.* 2007;27:211–219.

27. Jarmar T, Palmquist A, Brånemark R, et al. Characterization of the surface properties of commercially available dental implants using scanning electron microscopy, focused ion beam, and high-resolution transmission electron microscopy. *Clin Implant Dent Relat Res.* 2008;10:11–22.

28. Kanagaraja S, Lundström I, Nygren H, et al. Platelet binding and protein adsorption to titanium and gold after short time exposure to heparinized plasma and whole blood. *Biomaterials*. 1996;17:2225–2232.

29. Puleo DA, Nanci A. Understanding and controlling the bone implant interface. *Biomaterials*. 1999;20:2311–2321.

30. Park JY, Gemmell CH, Davies JE. Platelet interactions with titanium: Modulation of platelet activity by surface topography. *Biomaterials*. 2001;22:2671–2682.

31. An YH, Friedman RJ. Animal selections in orthopaedic research. In: An YH, Friedman RJ, ed. *Animal Models in Orthopaedic Research*. Boca Raton, FL: CRC Press LLC; 1999:39–57.

32. Thorwarth M, Schultze-Mosgau S, Kessler P, et al. Bone regeneration in osseous defects using a resorbable nanoparticular hydroxyapatite. *J Oral Maxillofac Surg.* 2005;63:1626–1633.

33. Pearce AI, Richards LG, Milz S, et al. Animal models for implant biomaterial research in bone: A review. *Eur Cell Mater.* 2007;13:1–10.

34. Mosekilde L, Kragstrup J, Richards A. Compressive strength, ash weight, and volume of vertebral trabecular bone in experimental fluorosis in pigs. *Calcif Tissue Int.* 1987;40:318–322.

35. Aerssens J, Boonen S, Lowet G, et al. Interspecies differences in bone composition, density, and quality: Potential implications for in vivo bone research. *Endocrinology*. 1998;139: 663–670.

36. Schierano G, Canuto RA, Navone R, et al. Biological factors involved in the osseointegration of oral titanium implants with different surfaces: A pilot study in minipigs. *J Periodontol.* 2005;76: 1710–1720.

37. Mosekilde L, Weisbrode SE, Safron JA, et al. Calcium-restricted ovariectomized Sinclair S-1 minipigs: An animal model of osteopenia and trabecular plate perforation. *Bone*. 1993; 14:379–382.

38. Kragstrup J, Richards A, Fejerskov O. Effects of fluoride on cortical bone remodeling in the growing domestic pig. *Bone*. 1989;10:421–424.

39. Buser D, Schenk RK, Steinemann S, et al. Influence of surface characteristics on bone integration of titanium implants. A histomorphometric study in miniature pigs. *J Biomed Mater Res.* 1991;25:889–902.

40. Preti G, Martinasso G, Peirone B, et al. Cytokines and growth factors involved in the osseointegration of oral titanium implants positioned using piezoelectric bone surgery versus a drill technique: A pilot study in minipigs. *J Periodontol.* 2007;78:716–722.

41. Depprich R, Zipprich H, Ommerborn M, et al. Osseointegration of zirconia implants compared with titanium: An in vivo study. *Head & Face Med*. 2008;4:30.

42. Ito Y, Sato D, Yoneda S, et al. Relevance of resonance frequency analysis to evaluate dental implant stability: Simulation and histomorphometrical animal experiments. *Clin Oral Implants Res.* 2008; 19:9–14.

43. Eom TG, Jeon GR, Jeong CM, et al. Experimental study of bone response to hydroxyapatite coating implants: Bone-implant contact and removal torque test. *Oral Surg Oral Med Oral Pathol Oral Radiol.* 2012;114:411–418.

44. Navarro M, Pu F, Hunt JA. The significance of the host inflammatory response on the therapeutic efficacy of cell therapies utilizing human adult stem cells. *Exp Cell Res.* 2012;318:361–370.

45. Kovach TK, Dighe AS, Lobo PI, et al. Interactions between MSCs and immune cells: Implications for bone healing. *J Immunol Res.* 2015;2015: 752510.

46. Xiao W, Wang Y, Pacios S. Cellular and molecular aspects of bone remodeling. *Front Oral Biol.* 2016;18:9–16.

47. Thevenot P, Hu W, Tang L. Surface chemistry influences implant biocompatibility. *Curr Top Med Chem.* 2008;8:270–280.

48. Kamath S, Bhattacharyya D, Padukudru C, et al. Surface chemistry influences implant-mediated host tissue responses. *J Biomed Mater Res A.* 2008; 86:617–626.

49. Varoni E, Canciani E, Palazzo B, et al. Effect of Poly-L-Lysine coating on titanium osseointegration: From characterization to in vivo studies. *J Oral Implantol.* 2015;41:626–631.

50. Hallab NJ, Jacobs JJ. Biologic effects of implant debris. *Bull NYU Hosp Jt Dis.* 2009;67:182–188.

51. Harder S, Quabius ES, Ossenkop L, et al. Surface contamination of dental implants assessed by gene expression analysis in a whole-blood in vitro assay: A preliminary study. *J Clin Periodontol.* 2012;39:987–994.

52. Lee J, Hurson S, Tadros H, et al. Crestal remodelling and osseointegration at surface-modified commercially pure titanium and titanium alloy implants in a canine model. *J Clin Periodontol.* 2012;39:781–788.

53. Lin A, Wang CJ, Kelly J, et al. The role of titanium implant surface modification with hydroxyapatite nanoparticles in progressive early bone-implant fixation in vivo. *Int J Oral Maxillofac Implants.* 2009;24:808–816.

54. Kohles SS, Clark MB, Brown CA, et al. Direct assessment of profilometric roughness variability from typical implant surface types. *Int J Oral Maxillofac Implants.* 2004;19:510–516.

55. Albrektsson T, Wennerberg A. Oral implant surfaces: Part 1–review focusing on topographic and chemical properties of different surfaces and in vivo responses to them. *Int J Prosthodont.* 2004;17:536–543.